

# Bifurcation analysis of the reduced model of the Bray–Liebhafsky reaction

Stevan Maćešić<sup>1</sup> · Željko Čupić<sup>2</sup> · Ljiljana Kolar-Anić<sup>1,2</sup>

Received: 22 December 2015 / Accepted: 13 February 2016 / Published online: 27 February 2016  
© Akadémiai Kiadó, Budapest, Hungary 2016

**Abstract** In this paper, an already published model of the Bray–Liebhafsky reaction was improved by removing the direct autoinhibitory step, which resulted in a new variant of the model with more realistic kinetic scheme than the earlier version. The obtained variant of the model retains all intermediate species ( $I^-$ , HIO, HIO<sub>2</sub> and I<sub>2</sub>) that were present in the previous model and has one reaction less. Stability analysis of the improved model was performed by stoichiometric network analysis (SNA). By this method, it was shown that improved model can simulate Andronov–Hopf and saddle-node bifurcations. In order to confirm the results of SNA, bifurcation analysis was performed with the initial concentrations of  $[H_2O_2]_0$  as the control parameter. With selected set of rate constants and constant concentrations of external species, two Andronov–Hopf bifurcations were detected at  $[H_2O_2]_0 = 5.62 \times 10^{-2}$  M and  $[H_2O_2]_0 = 10.73$  M, while the rate constants ought to be changed for a saddle-node to occur. Bifurcation analysis also showed that the interaction between intermediate species  $I^-$ , HIO and HIO<sub>2</sub> has a crucial impact on the emergence of Andronov–Hopf bifurcation.

**Keywords** Bifurcation analysis · Andronov–Hopf bifurcation · Bray–Liebhafsky oscillatory reaction · Stoichiometric network analysis (SNA) · Steady state stability

---

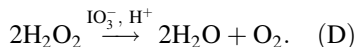
✉ Stevan Maćešić  
stevan.macesic@ffh.bg.ac.rs

<sup>1</sup> Faculty of Physical Chemistry, University of Belgrade, Studentski trg 12-16, 11158 Belgrade, Serbia

<sup>2</sup> Department of Catalysis and Chemical Engineering, Institute of Chemistry, Technology and Metallurgy, University of Belgrade, Njegoševa 12, 11000 Belgrade, Serbia

## Introduction

The Bray–Liebhafsky (BL) [1, 2] reaction is the decomposition (D) of hydrogen peroxide in the presence of iodate and hydrogen ions, which can be presented by the following simple net process



However, multiple intermediary species such as  $\text{I}_2$ ,  $\text{I}^-$ ,  $\text{HIO}$ ,  $\text{HIO}_2$  and  $\text{I}_2\text{O}$  are involved in the complex reaction network underlying this schematic representation [1–8]. Therefore, beside simple oscillations in concentrations of these intermediary species, complex oscillations and chaos are also obtained in this reaction system. [9–11]

Modelling of the BL reaction is a very complicated task due to complexity of the considered process. Several models and their variants of the BL reaction were proposed, among which model M(1-8) [3, 4, 12–15] showed the best performances.

Numerical investigations of model M(1-8) have shown that this model can simulate various types of periodic and aperiodic oscillatory dynamics [7, 12, 15–17], which were all found in experiments [9, 18]. However, the direct mathematical correlation between experimental results and numerical simulations is not simple due to the complexity of the model in terms of reaction network and chemical species. Thus, a better understanding of reactions and interactions between intermediate species, which are essential for emergence of instabilities, requires reduction of the considered model to both the number of intermediate species and the set of reactions, which represent the unstable core.

For this purpose, stoichiometric network analysis (SNA) [19, 20] was already applied to model M(1-8), which resulted in removing intermediate species ( $\text{I}_2\text{O}$ ) and in new model [21, 22]. The obtained model without one intermediate species ( $\text{I}_2\text{O}$ ), is presented in Table 1.

The number of reactions ( $R_i$ ) are adjusted with the number of reactions in model M(1-8) [21, 22]. The concentration  $[\text{H}^+] = 0.049 \text{ M}$  and  $[\text{IO}_3^-] = 0.0733$  are

**Table 1** Model M1 of the Bray–Liebhafsky reaction [21, 22]

$\text{IO}_3^- + \text{I}^- \rightleftharpoons \text{HIO} + \text{HIO}_2$	$k_1 = 55.96 \text{ min}^{-1}$	(R1)
	$k_{-1} = 7.91 \times 10^7 \text{ M}^{-1} \text{ min}^{-1}$	(R-1)
$\text{HIO} + \text{I}^- \rightleftharpoons \text{I}_2 + \text{H}_2\text{O}$	$k_4 = 3.00 \times 10^{11} \text{ M}^{-1} \text{ min}^{-1}$	(R4)
	$k_{-4} = 91.83 \text{ min}^{-1}$	(R-4)
$\text{HIO} + \text{I}^- \longrightarrow \text{I}^- + \text{H}^+ + \text{O}_2 + \text{H}_2\text{O}$	$k_5 = 1.34 \times 10^4 \text{ M}^{-1} \text{ min}^{-1}$	(R5)
$\text{HIO}_2 + \text{H}_2\text{O}_2 \longrightarrow \text{IO}_3^- + \text{H}^+ + \text{H}_2\text{O}$	$k_7 = 2.00 \times 10^3 \text{ M}^{-1} \text{ min}^{-1}$	(R7)
$\text{IO}_3^- + \text{H}^+ + \text{H}_2\text{O}_2 \longrightarrow \text{HIO}_2 + \text{O}_2 + \text{H}_2\text{O}$	$k_8 = 2.10 \times 10^{-4} \text{ min}^{-1}$	(R8)
$\text{HIO}_2 + \text{I}^- + \text{H}^+ \longrightarrow 2\text{HIO}$	$k_9 = 2.45 \times 10^{10} \text{ M}^{-1} \text{ min}^{-1}$	(R9)
$\text{HIO}_2 + \text{I}^- + \text{H}^+ + \text{H}_2\text{O}_2 \longrightarrow \text{HIO} + \text{HIO}_2 + \text{H}_2\text{O}$	$k_{10} = 2.45 \times 10^{10} \text{ M}^{-1} \text{ min}^{-1}$	(R10)
$2\text{HIO} + \text{H}_2\text{O}_2 \longrightarrow \text{HIO} + \text{HIO}_2 + \text{H}_2\text{O}$	$k_{11} = 3.15 \times 10^{10} \text{ M}^{-1} \text{ min}^{-1}$	(R11)

considered to be constant and they are incorporated into the values of the appropriate rate constants.

In a previous work [21], it was shown that this model can simulate oscillatory dynamic states, either in the complete form  $M(1, -1, 4, -4, 5, 7, 8, 9, 10, 11)$  or without some of the reactions, that is in the forms:  $M(1, -1, 4, -4, 5, 7, 8, 9, 11)$ ,  $M(1, -1, 4, -4, 5, 9, 11)$  and  $M(4, -4, 5, 7, 8, 9, 11)$ . Thus, by a systematic contracting procedure, the variant of the model  $M(1, -1, 4, -4, 5, 9, 11)$ , already published by Guy Schmitz, is also obtained [23]. The contracted model M1 is here reconstructed by the method proposed by Cook et al. [24] with the aim to escape a direct autoinhibitory step that appears in reaction R11 and which cannot be considered as part of a realistic kinetic mechanism. Moreover, the obtained domain of instability, dynamic states, bifurcation diagrams, and type of bifurcations are calculated and discussed for the new variant of the model. For this purpose, beside SNA, the methods of numerical continuation [25–30] was also used.

## Methods

### Stoichiometric network analysis

Stoichiometric network analysis (SNA) is a powerful and efficient method for carrying out stability and reaction route analysis of complex reaction systems including biochemical ones. This method allows the evaluation of stability and the derivations of analytical expressions for instability conditions without the need of knowing the values of kinetic parameters that are usually experimentally inaccessible.

In SNA, the kinetic equations of any stoichiometric model are represented by a set of differential kinetic equations written in the matrix form:

$$\frac{dc}{dt} = \mathbf{S}\mathbf{r} \tag{1}$$

Here  $\mathbf{c}$  is the concentration, while  $\mathbf{r}$  is a reaction rate vector. The stoichiometric matrix  $\mathbf{S}$  is an operator whose elements are the stoichiometric coefficients  $S_{n,m}$  of compounds  $n$  in reaction  $m$ .

Stability analysis in SNA is based on the determination of the steady state stability and steady state reaction rates for the considered model. The rates at a steady state  $\mathbf{r}_{ss}$  are solutions of the relation

$$\mathbf{S}\mathbf{r}_{ss} = 0 \tag{2}$$

Here  $\mathbf{S}$  is stoichiometric matrix consisting of only independent intermediate species. Moreover, the overall process can be represented as a linear combination of several elementary reaction pathways with non-negative coefficients. These elementary reaction pathways are known as extreme currents  $E_i$  and they all contribute to the steady state values of reaction rates. The contributions of the extreme currents  $E_i$ , denoted as the current rates  $j_i$ , are the components of the corresponding current rate

vector  $\mathbf{j}$ , whereas the extreme currents  $E_i$  are the columns of the extreme current matrix  $\mathbf{E}$ . [19, 20, 31]

The basic equation of SNA, which gives a relation between steady state reaction rates and current rates is

$$\mathbf{r}_{ss} = \mathbf{E}\mathbf{j} \quad (3)$$

The steady-state stability is determined by analyzing the eigenvalues of the Jacobian of the system, which in SNA has the form [19, 20, 31]

$$\mathbf{M} = -\mathbf{V}(\mathbf{j}) \text{diag } \mathbf{h} \quad (4)$$

Here  $\mathbf{h}$  stands for the vector of reciprocal steady-state concentrations of the intermediate species,  $\text{diag } \mathbf{h}$  is its diagonal matrix, while  $\mathbf{V}(\mathbf{j})$  is a current rate matrix. It is given by the expression:

$$\mathbf{V}(\mathbf{j}) = -\mathbf{S} \text{diag} (\mathbf{E}\mathbf{j})\mathbf{K}^T \quad (5)$$

Here  $\mathbf{K}$  stands for a matrix of the order of reactions. If we assume the mass action law for the reaction rates, the elements of  $\mathbf{K}$  are the general stoichiometric coefficients of a species standing on the left side of the reaction (reactants in particular reactions), while  $\mathbf{K}^T$  is its transpose.

The eigenvalues of  $\mathbf{M}$  are the roots  $\lambda$  of the characteristic polynomial

$$\text{Det}[\lambda\mathbf{I} - \mathbf{M}] = \sum_{i=0}^n \alpha_i \lambda^{n-i} \quad (6)$$

If the real parts of all eigenvalues are negative, a steady state is stable. If one or more eigenvalues have positive real parts, the steady state is unstable.

The sign of the real part of the eigenvalues of the Jacobian matrix can be evaluated by using several criteria such as Hurwitz determinants [32, 33] or the  $\alpha$  approximation (a system is unstable if at least one coefficient of the characteristic polynomial  $\alpha$  is negative). Since our main goal is to derive an equation which gives us an instability condition, the two mentioned criteria are impractical to use because the equations derived for large models consist of hundreds or even thousands of terms. A much simpler method to examine the steady-state stability is the use of the matrix of current rates  $\mathbf{V}(\mathbf{j})$ . The steady state is considered unstable if there is at least one negative diagonal minor of  $\mathbf{V}(\mathbf{j})$ . [19] It is possible only if the polynomial corresponding to the determinant of the mentioned negative diagonal minor contain, at least, one negative term. Namely, a negative minor actually represents a destabilizing term since all the coefficients of the current rates in the  $\mathbf{V}(\mathbf{j})$  matrix are positive numbers. For a system to be able to simulate an Andronov–Hopf bifurcation, it is usually necessary that there is at least one negative diagonal minor of dimension  $(n - 1) \times (n - 1)$ , where  $n$  represents the number of intermediate species. The condition for a saddle-node bifurcation is that the expression for the determinant of  $\mathbf{V}(\mathbf{j})$  contains negative terms. Although it is an approximation, this criterion often gives very good results. [14, 34–37]

In order to compare the derived instability conditions, which are given as the functions of the current rates, with experimental and numerical results, they have to be expressed as the functions of reaction rates. To achieve this, matrix  $\mathbf{V}$  has to be calculated again but now using relation [38]

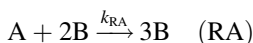
$$\mathbf{V}(\mathbf{r}_{ss}) = -\mathbf{S} \text{diag}(\mathbf{r}_{ss})\mathbf{K}^T \tag{7}$$

However, the preliminary identification of negative minors from the current rate matrix in the form 5 remains necessary. The form given in Eq. 7 is useful only for comparison with experiments.

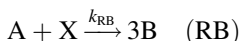
**Cook method**

Direct autocatalytic steps can often be found in the models of the oscillating reactions, but they cannot be considered as a realistic kinetic mechanism. Thus, replacing them with a realistic mechanism is an essential part of modelling oscillating reactions.

For achieving this goal, a procedure proposed by Cook et al. [24] can be used. The procedure consists of replacing direct autocatalytic steps



with a realistic sub-scheme, i.e., a set of elementary steps which preserve overall stoichiometry. In their paper, they proposed several such schemes, but for the purpose of this paper, we used the following sub-scheme:



Reactions RC and R–C describe fast equilibrium whereas much slower process RB is the rate limiting step in this sequence. Hence, the concentration  $[X]$  in the steady state is determined by the equilibrium reactions RC and R–C as  $K[B]^2$ :

$$[X] = \frac{k_{RC}[B]^2}{(k_{RB}[A] + k_{R-C})} \approx \frac{k_{RC}}{k_{R-C}} [B]^2 = K[B]^2 \tag{8}$$

Here  $K = k_{RC}/k_{R-C}$ . Therefore, the rate of the overall process has the form  $k_{RB} \cdot K[A][B]^2$ . Taking  $k_{RA} = k_{RB}K$ , the rate laws of two processes are equal. Thus, the cubic autocatalytic reaction is decomposed in its bimolecular steps and reaction kinetics is preserved. It is done by means of intermediate X, as a new species in submodel [RB, RC, R–C].

**Numerical continuation**

Numerical continuation is a method of computing approximate solutions of a system of parameterized nonlinear equations which can be represented in a form

$$f(\mathbf{c}, k) = 0 \quad (9)$$

Here  $\mathbf{c}$  represents concentration vector of size  $n \times 1$ , while  $k$  represents control parameters, which in our case are rate constants. By solving system 9 for various values of the chosen control parameter while others are kept constant, the dependence of the solution on the control parameter is obtained. By evaluating the eigenvalues of the Jacobian matrix for each value of control parameter, the stability of the system is evaluated. For the detection of bifurcation points which can be found in the considered system, test functions are used. A unique feature for all test functions is that they equal to zero in the bifurcation point. Bifurcations points are detected by monitoring the values of test functions for each value of the control parameter and detecting the point at which the test function changes its sign. [28, 29]

For the purpose of this research, we developed a program in MATLAB programming package which conducts bifurcation analysis by using numerical continuation based on the pseudo-arc length scheme.

## Results and discussion

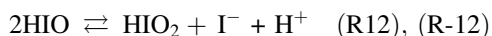
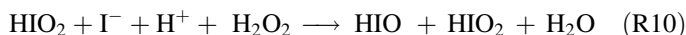
### Contraction of the model M1

After the successful removal of  $\text{I}_2\text{O}$  from the initial model M(1-8) by systematic contracting procedure performed by SNA, we obtained a model with a direct autoinhibitory step R11, which can be a source of instability as any feedback reaction, but which cannot be considered as a realistic kinetic mechanism and, therefore, must be substituted by two or more simpler reactions. In order to solve this problem, we accepted the procedure which Cook et al. applied on the autocatalyst in order to replace autocatalysis with a bimolecular steps (Section 2.2). With approximations described in Section 2.2, this procedure can be obviously valid for any process of the form



Here  $n = 1, 2, 3, \dots$ . Thus, it can be also applied on autoinhibition.

According to procedure explained in Section 2.2, reaction R11 can be replaced with following reactions



These have similar roles to reactions RB and RC together with R–C. Reaction R10, already included in model M1, should be a slow, rate determining step in accordance with the known facts about kinetics of iodide reaction with hydrogen peroxide. The stoichiometry of the fast equilibrium R12, R-12 also corresponds to well known process, which was an integral part of several previously published models of the BL reaction. Thus, from model M1, we can see that reaction R10 is already

present in it while reaction R11 needs to be replaced with equilibrium reaction R10, R-12. Also, the new reaction R-12 is identical to reaction R9, which should be replaced with it. Hence, in the new reduced model M2, (Table 2) submodel consisting of reactions R9, R10 and R11 is replaced with submodel consisting of reactions R10, R12 and R-12. In this procedure, when the direct autoinhibitory step is replaced with bimolecular steps in the submodel, we introduced iodide ion as new intermediate species. However, this is an already existing intermediate in the model such that number of intermediate species did not change.

Replacing reaction R11 with the set of reactions R10, R12 and R-12 requires adjustments in the values of rate constants in order to maintain the reaction rates. Due to the contribution of the decomposed autoinhibitory step R11, reactions R10 and R-12 would have to appear twice in the reaction scheme (since reaction R-12 is identical to the reaction R9), and this is equivalent to having the same reactions with doubled reaction rates, or doubled rate constants. Thus, values of  $k_{10}$  and  $k_{-12}$  are twice as high as their values in model M1 (namely,  $k_{-12} = 2k_9$ ). On the other hand, in order to preserve existing kinetics, it is required that reaction rate of R12 should be equal to the reaction rate of R11. Thus,  $k_{12}$  has the same value as  $k_{11}$  in model M1, but the rate of reaction R12 is larger than rate of reaction R11 since the last one is multiplied by hydrogen peroxide concentration, which is usually less than 1 M. However, low hydrogen peroxide concentration is not a necessary condition for oscillations, but rather the frame for the equivalency between two models. Therefore, replaced submodel R9, R10, R11 should be equivalent to the new one R10, R12, R-12 with a chemically realistic stoichiometry.

Model M2 consist of seven reactions, among which three are reversible. The first five reactions are the same as in model M(1-8), while the last two reactions are obtained during the process of contraction.

The dynamics of the Model M2 can be represented by a set of ordinary differential kinetic equations:

$$\frac{d[I^-]}{dt} = -r_1 + r_{-1} - r_4 + r_{-4} + r_5 - r_{10} + r_{12} - r_{-12} \tag{11}$$

**Table 2** Model M2 of the Bray–Leibhafsky reaction

$IO_3^- + I^- + 2H^+ \rightleftharpoons HIO + HIO_2$	$k_1 = 55.96 \text{ min}^{-1}$	(R1)
	$k_{-1} = 7.91 \times 10^7 \text{ M}^{-1} \text{ min}^{-1}$	(R-1)
$HIO + I^- + H^+ \rightleftharpoons I_2 + H_2O$	$k_4 = 3.00 \times 10^{11} \text{ M}^{-1} \text{ min}^{-1}$	(R4)
	$k_{-4} = 91.83 \text{ min}^{-1}$	(R-4)
$HIO + H_2O_2 \longrightarrow I^- + H^+ + O_2 + H_2O$	$k_5 = 1.34 \times 10^4 \text{ M}^{-1} \text{ min}^{-1}$	(R5)
$HIO_2 + H_2O_2 \longrightarrow IO_3^- + H^+ + H_2O$	$k_7 = 2.00 \times 10^3 \text{ M}^{-1} \text{ min}^{-1}$	(R7)
$IO_3^- + H^+ + H_2O_2 \longrightarrow HIO_2 + O_2 + H_2O$	$k_8 = 2.10 \times 10^{-4} \text{ min}^{-1}$	(R8)
$HIO_2 + I^- + H^+ + H_2O \rightarrow HIO + HIO_2 + H_2O$	$k_{10} = 4.90 \times 10^{10} \text{ M}^{-1} \text{ min}^{-1}$	(R10)
$2HIO \rightleftharpoons HIO_2 + I^- + H^+$	$k_{12} = 3.15 \times 10^{10} \text{ M}^{-1} \text{ min}^{-1}$	(R12)
	$k_{-12} = 4.90 \times 10^{10} \text{ M}^{-1} \text{ min}^{-1}$	(R-12)

$$\frac{d[\text{HIO}]}{dt} = r_1 - r_{-1} - r_4 + r_{-4} - r_5 + r_{10} - 2 r_{12} + 2 r_{-12} \quad (12)$$

$$\frac{d[\text{HIO}_2]}{dt} = r_1 - r_{-1} - r_7 + r_8 + r_{12} - r_{-12} \quad (13)$$

$$\frac{d[\text{I}_2]}{dt} = r_4 - r_{-4} \quad (14)$$

Here  $r_i$  are defined as

$$r_1 = k_1[\text{I}^-] \quad (15)$$

$$r_{-1} = k_{-1}[\text{HIO}][\text{HIO}_2] \quad (16)$$

$$r_4 = k_4[\text{I}^-][\text{HIO}] \quad (17)$$

$$r_{-4} = k_{-4}[\text{I}_2] \quad (18)$$

$$r_5 = k_5[\text{HIO}][\text{H}_2\text{O}_2]_0 \quad (19)$$

$$r_7 = k_7[\text{HIO}_2][\text{H}_2\text{O}_2]_0 \quad (20)$$

$$r_8 = k_8[\text{H}_2\text{O}_2]_0 \quad (21)$$

$$r_{10} = k_{10}[\text{HIO}_2][\text{I}^-][\text{H}_2\text{O}_2]_0 \quad (22)$$

$$r_{12} = k_{12}[\text{HIO}]^2 \quad (23)$$

$$r_{-12} = k_{-12}[\text{HIO}_2][\text{I}^-] \quad (24)$$

Here, as in all previous variants of model M(1-8), the concentrations of  $\text{H}^+$  and  $\text{IO}_3^-$  are considered to be constant and their values are incorporated in the values of appropriate rate constants. For the purpose of the numerical simulations, stability analysis and bifurcation analysis, the concentration of  $[\text{H}_2\text{O}_2]$  is considered to be constant and equal to the initial  $[\text{H}_2\text{O}_2]_0$ . Therefore, there is  $[\text{H}_2\text{O}_2]_0$  instead of  $[\text{H}_2\text{O}_2]$  in expressions for  $r_5$ ,  $r_7$ ,  $r_8$  and  $r_{10}$ .

### Stability analysis of the model M2

As has just been explained, in model M2, there are four intermediate species:  $\text{I}^-$ ,  $\text{HIO}$ ,  $\text{HIO}_2$  and  $\text{I}_2$ , which is one fewer than in model M(1–8) and seven reactions among which three are reversible. For stability analysis, we are dealing with ten forward reactions, since any reverse one had to be presented as two forward ones.

The first step in stability analysis is to construct matrices **S** and **K**, in which columns represents reactions while rows represent intermediate species



$$\mathbf{S} = \begin{matrix} & R_1 & R_{-1} & R_4 & R_{-4} & R_5 & R_7 & R_8 & R_{10} & R_{12} & R_{-12} \\ \begin{bmatrix} -1 & 1 & -1 & 1 & 1 & 0 & 0 & -1 & 1 & -1 \\ 1 & -1 & -1 & 1 & -1 & 0 & 0 & 1 & -2 & 2 \\ 1 & -1 & 0 & 0 & 0 & -1 & 1 & 0 & 1 & -1 \\ 0 & 0 & 1 & -1 & 0 & 0 & 0 & 0 & 0 & 0 \end{bmatrix} & \begin{matrix} \Gamma^- \\ \text{HIO} \\ \text{HIO}_2 \\ \text{I}_2 \end{matrix} \end{matrix} \tag{25}$$

$$\mathbf{K} = \begin{matrix} & R_1 & R_{-1} & R_4 & R_{-4} & R_5 & R_7 & R_8 & R_{10} & R_{12} & R_{-12} \\ \begin{bmatrix} 1 & 0 & 1 & 0 & 0 & 0 & 0 & 1 & 0 & 1 \\ 0 & 1 & 1 & 0 & 1 & 0 & 0 & 0 & 2 & 0 \\ 0 & 1 & 0 & 0 & 0 & 1 & 0 & 1 & 0 & 1 \\ 0 & 0 & 0 & 1 & 0 & 0 & 0 & 0 & 0 & 0 \end{bmatrix} & \begin{matrix} \Gamma^- \\ \text{HIO} \\ \text{HIO}_2 \\ \text{I}_2 \end{matrix} \end{matrix} \tag{25}$$

Then matrix **E** is calculated for the model M2

$$\mathbf{E} = \begin{matrix} & E_1 & E_2 & E_3 & E_4 & E_5 & E_6 & E_7 \\ \begin{bmatrix} 1 & 0 & 0 & 0 & 0 & 1 & 0 \\ 1 & 0 & 0 & 0 & 0 & 0 & 1 \\ 0 & 1 & 0 & 0 & 0 & 0 & 0 \\ 0 & 1 & 0 & 0 & 0 & 0 & 0 \\ 0 & 0 & 1 & 0 & 0 & 1 & 0 \\ 0 & 0 & 0 & 0 & 1 & 1 & 0 \\ 0 & 0 & 0 & 0 & 1 & 0 & 1 \\ 0 & 0 & 1 & 0 & 0 & 0 & 1 \\ 0 & 0 & 0 & 1 & 0 & 0 & 0 \\ 0 & 0 & 0 & 1 & 0 & 0 & 0 \end{bmatrix} & \begin{matrix} R_1 \\ R_{-1} \\ R_4 \\ R_{-4} \\ R_5 \\ R_7 \\ R_8 \\ R_{10} \\ R_{12} \\ R_{-12} \end{matrix} \end{matrix} \tag{27}$$

By employing Eq. 3, relations between current rates and reaction rates  $r_{ss}$  at steady state are obtained. Indexes SS indicating that reaction rate values are taken in the steady state are excluded from all equations below for simplicity, but this fact must be kept in mind.

$$r_1 = j_1 + j_6 \tag{28}$$

$$r_{-1} = j_1 + j_7 \tag{29}$$

$$r_4 = j_2 \tag{30}$$

$$r_{-4} = j_2 \tag{31}$$

$$r_5 = j_3 + j_6 \quad (32)$$

$$r_7 = j_5 + j_6 \quad (33)$$

$$r_8 = j_5 + j_7 \quad (34)$$

$$r_{10} = j_3 + j_7 \quad (35)$$

$$r_{12} = j_4 \quad (36)$$

$$r_{-12} = j_4 \quad (37)$$

By using Eq. 5, matrix  $\mathbf{V}(\mathbf{j})$  was calculated:

$$\mathbf{V}(\mathbf{j}) = \begin{array}{cccc} & \Gamma & \text{HIO} & \text{HIO}_2 & \text{I}_2 \\ \left[ \begin{array}{cccc} j_1 + j_2 + j_3 + j_4 + j_6 + j_7 & -j_1 + j_2 - j_3 - 2j_4 - j_6 - j_7 & -j_1 + j_3 + j_4 & -j_2 \\ -j_1 + j_2 - j_3 - 2j_4 - j_6 - j_7 & j_1 + j_2 + j_3 + 4j_4 + j_6 + j_7 & j_1 - j_3 - 2j_4 & -j_2 \\ -j_1 + j_4 - j_6 & j_1 - 2j_4 + j_7 & j_1 + j_4 + j_5 + j_6 + j_7 & 0 \\ -j_2 & -j_2 & 0 & j_2 \end{array} \right] & \begin{array}{l} \Gamma \\ \text{HIO} \\ \text{HIO}_2 \\ \text{I}_2 \end{array} \end{array} \quad (38)$$

Analysis of diagonal minors of dimensions  $i \times i$  of matrix  $\mathbf{V}(\mathbf{j})$  showed that there are four of them that negative determinant terms. They are given in Table 3, where particular numbers  $i$  correspond to the rows and columns of negative minors.

The steady state is considered unstable if there is at least one negative diagonal minor of  $\mathbf{V}(\mathbf{j})$ . [19] It is possible only if the polynomial corresponding to the determinant of the mentioned negative diagonal minor contain at least one negative term. Namely, a negative minor actually represents a destabilizing term since all the coefficients of the current rates in the  $\mathbf{V}(\mathbf{j})$  matrix are positive numbers. For a system to be able to simulate an Andronov–Hopf bifurcation, it is usually necessary that there is at least one negative diagonal minor of dimension  $(n - 1) \times (n - 1)$ , where  $n$  represents the number of intermediate species. The condition for a saddle-node bifurcation is that the expression for the determinant of  $\mathbf{V}(\mathbf{j})$  contains negative terms. Although it is an approximation, this criterion often gives very good results. [14, 34–37]

**Table 3** Negative diagonal minors of matrix  $\mathbf{V}(\mathbf{j})$  for model M2. Dimensions of minors are given in the first column and the corresponding combination of rows-columns of matrix  $\mathbf{V}(\mathbf{j})$  is indicated by a plus sign in other columns

Dimensions of minors	1 ( $\Gamma$ )	2 (HIO)	3 (HIO <sub>2</sub> )	4 (I <sub>2</sub> )
2 × 2		+	+	
3 × 3	+	+	+	
3 × 3		+	+	+
4 × 4	+	+	+	+

In the first row of Table 3, columns and rows of matrix  $\mathbf{V}(\mathbf{j})$  are identified by ordinal numbers together with corresponding intermediary species denoted on the borders of matrix  $\mathbf{V}(\mathbf{j})$  (38)

As we already said in Section 2.1, the steady state is unstable if at least one of the polynomials corresponding to the determinants of the negative diagonal minors of matrix  $\mathbf{V}(\mathbf{j})$  can be negative in the considered region of parameters. [19] However, the Andronov–Hopf bifurcation can be obtained only if there is at least one negative diagonal minor of dimension  $(n - 1) \times (n - 1)$ , where  $n$  represents the number of intermediate species. In our case, there are two of them. Moreover, since the considered model has four intermediate species, we are looking for negative diagonal minors of dimension  $4 \times 4$  as a condition for the appearance of a saddle-node bifurcation.

Now, if we continue with the analysis of diagonal minors, we can see that the smallest one is of dimension  $2 \times 2$  and represents the interaction between HIO and HIO<sub>2</sub>. This minor is also incorporated into negative diagonal minors of dimension  $3 \times 3$  and  $4 \times 4$  and thus it represents the core of instability in model M2. The polynomial corresponding to minor  $2 \times 2$  is negative if

$$\begin{aligned}
 & j_1j_2 + 2j_1j_3 + 9j_1j_4 + j_1j_5 + j_2j_4 + 2j_1j_6 + j_2j_5 + j_1j_7 + j_2j_6 + j_3j_5 + j_2j_7 + j_3j_6 \\
 & + 4j_4j_5 + 2j_3j_7 + 5j_4j_6 + 7j_4j_7 + j_5j_6 + j_5j_7 + 2j_6j_7 + j_6^2 + j_7^2 - j_3j_4 < 0
 \end{aligned}
 \tag{39}$$

Since there are linear relations between current rates and reaction rates 15–24, this inequality can also be expressed as a function of  $r_{ss}$  [38]

$$\begin{aligned}
 & 4r_{12}r_7 + r_4r_7 + r_5r_7 + r_{-1}r_{10} + 6r_{-1}r_{12} + r_{-1}r_4 + r_4r_{-12} + r_{-1}r_5 + r_5r_{-12} + r_{-1}r_7 \\
 & + 3r_{-1}r_{-12} - 2r_{10}r_{12} < 0
 \end{aligned}
 \tag{40}$$

Expressions for minors of dimension  $3 \times 3$  ( $M_{123}$  and  $M_{234}$ ) as a function of  $r_{ss}$  are given in Eqs. 41 and 42:

$$\begin{aligned}
 & (2r_{10}r_{12} + 2r_4r_{10} + 2r_7r_{12} + 2r_4r_7 + 5r_4r_{-12})r_1 \\
 & + (2r_{10}r_{12} + 4r_4r_{10} + 10r_4r_{12} + 2r_4r_5 + 2r_4r_7 + 10r_4r_{-12} - r_7r_{-12})r_{-1} \\
 & + (3r_7r_{12} + r_5r_{-12} - 2r_{10}r_{12})2r_4 + (2r_{10}r_{12} + 2r_4r_{10} + 2r_4r_5 + 3r_4r_{-12})r_7 \\
 & - r_5r_{-12}(r_1 + r_{-1} + r_7) < 0
 \end{aligned}
 \tag{41}$$

$$\begin{aligned}
 & r_{-4}((r_5 + r_7 + r_{10} + 6r_{12} + 3r_{-12})r_{-1} + r_5(r_7 + r_{-12}) + (2r_7 - r_{10})2r_{12}) < 0
 \end{aligned}
 \tag{42}$$

Furthermore, the condition for the appearance of a saddle-node bifurcation resulting from minor  $4 \times 4$  can be expressed as

$$\begin{aligned}
 & r_{-4}(2r_{12}(r_1r_{10} + r_1r_7 + r_7r_{10} + r_{-1}r_{10}) - r_{-12}(r_1r_5 + r_5r_7 + r_{-1}r_5 + r_{-1}r_7)) = 0
 \end{aligned}
 \tag{43}$$

Since  $r_{-4}$  cannot be zero, condition 43 can be written in a form

$$\frac{2r_{12}}{r_{-12}} = \frac{r_5(r_1 + r_{-1} + r_7) + r_{-1}r_7}{r_{10}(r_1 + r_{-1} + r_7) + r_1r_7} \quad (44)$$

By setting proper values of the parameters, condition 43 can be satisfied and a saddle-node bifurcation will occur, while the best parameter to adjust in order for this to be achieved is rate constant  $k_{12}$ .

### Bifurcation analysis of the model M2

In order to confirm the results of SNA analysis of the model M2, the bifurcation analysis was carried out. To perform bifurcation analysis, Eq. 2, which governs the concentrations of intermediate species in steady-state had to be solved. In the case of model M2, those equations are:

$$-r_1 + r_{-1} - r_4 + r_{-4} + r_5 - r_{10} + r_{12} - r_{-12} = 0 \quad (45)$$

$$r_1 - r_{-1} - r_4 + r_{-4} - r_5 + r_{10} - 2r_{12} + 2r_{-12} = 0 \quad (46)$$

$$r_1 - r_{-1} - r_7 + r_8 + r_{12} - r_{-12} = 0 \quad (47)$$

$$r_4 - r_{-4} = 0 \quad (48)$$

Bifurcation analysis of the considered model was carried out with the initial concentration of hydrogen-peroxide  $[\text{H}_2\text{O}_2]_0$  as a bifurcation parameter. The value of the  $[\text{H}_2\text{O}_2]_0$  was varied in range  $1 \times 10^{-2} \text{ M} < [\text{H}_2\text{O}_2]_0 < 15 \text{ M}$ , while other rate constants were kept constant and for each value of hydrogen peroxide, steady-state concentrations of intermediate species were calculated. The stability of the system was determined by evaluating the eigenvalues of the Jacobian matrix for each value of the chosen rate constants, while the emergence of the bifurcation points was detected by evaluating appropriate test functions. The bifurcation diagram for parameters given in Table 2 is presented in Fig. 1.

By varying  $[\text{H}_2\text{O}_2]_0$ , two Andronov–Hopf bifurcations were detected at values  $\text{AH}_1([\text{H}_2\text{O}_2]_0 = 5.6289 \times 10^{-2} \text{ M})$  and  $\text{AH}_2([\text{H}_2\text{O}_2]_0 = 10.7387 \text{ M})$ . In order to determine which diagonal minor from Table 3 represents the most accurate expression

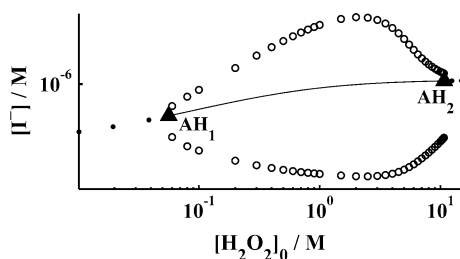
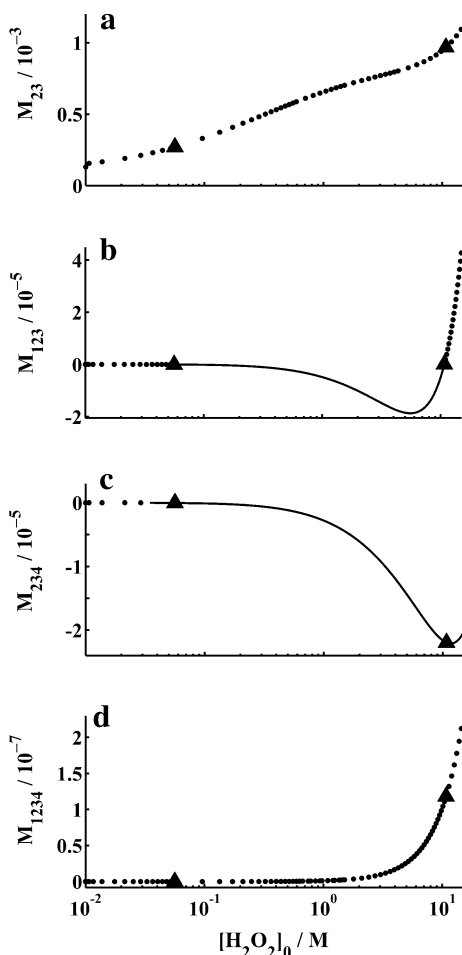


**Fig. 1** Bifurcation diagram obtained by solving Eqs. 45–48 with chosen initial concentrations of hydrogen-peroxide  $[\text{H}_2\text{O}_2]_0$ . In Fig. 1 dots denote stable-steady state, line denote unstable steady-state, filled triangles denote Andronov–Hopf bifurcations ( $\text{AH}_1$  and  $\text{AH}_2$ ) while circles denote amplitude of the oscillations—minimum and maximum values of iodide concentration in it. The abscissa and ordinate are given on a logarithmic scale

**Fig. 2** Values of the diagonal minors  $M_{23}$  (a),  $M_{123}$  (b),  $M_{234}$  (c), and  $M_{1234}$  (d) calculated for values of  $[H_2O_2]_0$  in the range  $1 \times 10^{-2} \text{ M} < [H_2O_2]_0 < 15 \text{ M}$  and rate constants given in Table 2. In Fig. 2 *dots* denote positive value of diagonal minors; *line* denotes negative value of diagonal minors; *filled triangles* denote Andronov–Hopf bifurcations. The abscissa is given on a logarithmic scale

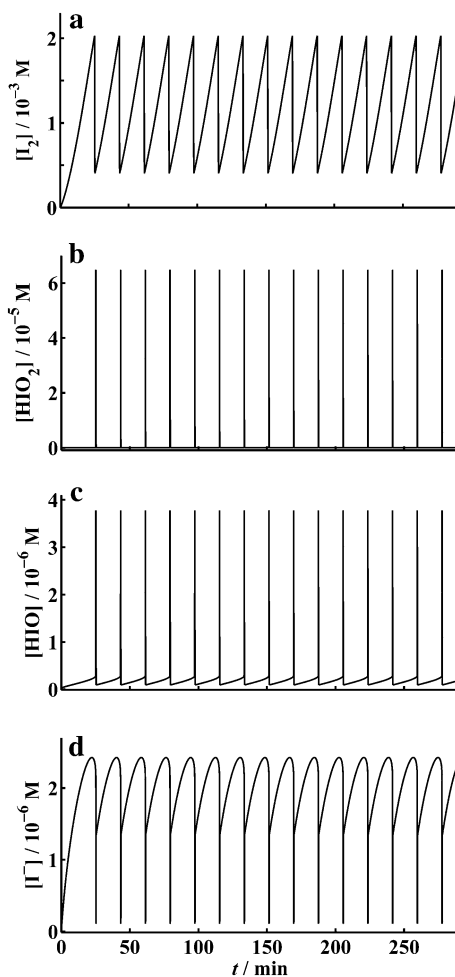


for the appearance of the Andronov–Hopf bifurcation under the considered conditions, we calculated their values for  $[H_2O_2]_0$  in the range of  $1 \times 10^{-2} \text{ M} < [H_2O_2]_0 < 15 \text{ M}$  and determined the values of  $[H_2O_2]_0$  for which they have negative values. By comparing the values of  $[H_2O_2]_0$  at which diagonal minors become negative and then positive again with the values of  $[H_2O_2]_0$  at which two Andronov–Hopf bifurcation were detected, we determined which diagonal minor is most important for the appearance of the considered bifurcation. The results are presented in Fig. 2.

From the results presented in Fig. 2 and obtained with the rate constants given in Table 2, we can see that diagonal minor  $M_{23}$ , although included in the diagonal minor  $M_{123}$  and  $M_{234}$ , cannot become negative in the analyzed range of  $[H_2O_2]_0$ . Therefore, the considered steady state cannot be unstable under the analyzed set of rate constants and initial concentrations of invariable species.

Diagonal minor  $M_{234}$  becomes negative at  $[H_2O_2]_0 = 3.4745 \times 10^{-2} \text{ M}$ , but it is still negative after  $AH_2([H_2O_2]_0 = 10.7387 \text{ M})$ . On the other hand, diagonal minor

**Fig. 3** Temporal evolution of the intermediate species  $I_2$ ,  $HIO_2$ ,  $HIO$  and  $I^-$  of the model M2. Simulations were carried out for the concentration of  $[H_2O_2] = 0.35$  M



$M_{123}$  becomes negative at  $[H_2O_2]_0 = 5.5748 \times 10^{-2}$  M and then positive at  $[H_2O_2]_0 = 10.7164$  M, and they are at good agreement with the values for  $AH_1$  and  $AH_2$ . Therefore, diagonal minor  $M_{123}$  gives the most accurate expression for the appearance of the Andronov–Hopf bifurcation in model M2. On the other hand, values of the minor  $M_{1234}$  are positive for the selected set of rate constants and any positive value of  $[H_2O_2]_0$ . Hence, for a saddle-node bifurcation to occur, rate constants have to be used as control parameters.

For all values of  $[H_2O_2]_0$  that satisfy condition 41, oscillatory dynamics must be obtained. As an example, we present results of a numerical simulation for  $[H_2O_2]_0 = 0.35$  M and the rate constants given in Table 2 (Fig. 3).

## Conclusion

The improved model of the BL reaction proposed by Cook et al. in order to replace autocatalysis with bimolecular steps in the case of autocatalysis is applied here on the already contracted model M1 of the Bray–Liebhafsky reaction with the aim to substitute the direct autoinhibitory reaction with two or more simpler reactions, e.g. with some more realistic ones. Thus, starting from contracted model M1 having formally eight reactions, where two of them are reverse ones, we obtained the improved model M2 with formally seven reactions, where three of them are reverse ones and without the direct autoinhibitory step. In this procedure, we did not introduce new intermediate species, but solved the problem by means of the already existing intermediate, iodide ion.

The improved model of the BL reaction (M2) was analyzed with SNA and it was found that this model can simulate Andronov–Hopf and saddle-node bifurcations. The bifurcation analysis of this model was carried out with the initial concentration of hydrogen-peroxide  $[H_2O_2]_0$  as the bifurcation parameter. By varying the control parameter in the range  $1 \times 10^{-2} \text{ M} < [H_2O_2]_0 < 15 \text{ M}$  while the values of all other parameters (rate constants and constant concentrations of external species) were fixed, two Andronov–Hopf bifurcations were detected. By analyzing negative diagonal minors, it was found that the core of instability is ordered by the concentrations of the following three intermediate species:  $I^-$ , HIO and HIO<sub>2</sub>.

**Acknowledgments** The present investigations were supported by The Ministry of Education, Science and Technological Development of the Republic of Serbia, under Project 172015 and 45001.

## References

1. Bray WC (1921) A periodic reaction in homogeneous solution and its relation to catalysis. *J Am Chem Soc* 43:1262–1267. doi:[10.1021/ja01439a007](https://doi.org/10.1021/ja01439a007)
2. Bray WC, Liebhafsky HA (1931) Reactions involving hydrogen peroxide, iodine and iodate ion. I: Introduction. *J Am Chem Soc* 53:38–44. doi:[10.1021/ja01352a006](https://doi.org/10.1021/ja01352a006)
3. Kolar-Anić Lj, Schmitz G (1992) Mechanism of the Bray–Liebhafsky reaction: effect of the oxidation of iodosic acid by hydrogen peroxide. *J Chem Soc Faraday Trans* 88:2343–2349. doi:[10.1039/FT9928802343](https://doi.org/10.1039/FT9928802343)
4. Kolar-Anić Lj, Misljenović D, Anić S, Nicolis G (1995) Influence of the reduction of iodate ion by hydrogen peroxide on the model of the Bray–Liebhafsky reaction. *React Kinet Catal Lett* 54:35–41. doi:[10.1007/BF02071178](https://doi.org/10.1007/BF02071178)
5. Kolar-Anić Lj, Misljenović D, Anić S (1996) Kinetic model for the Bray–Liebhafsky process without the reaction  $IO_3^- + I^- + 2H^+ \rightleftharpoons HIO + HIO_2$ . *React Kinet Catal Lett* 57:37–42. doi:[10.1007/BF02076117](https://doi.org/10.1007/BF02076117)
6. Kolar-Anić Lj, Čupić Ž, Anić S, Schmitz G (1997) Pseudo-steady states in the model of the Bray–Liebhafsky oscillatory reaction. *J Chem Soc Faraday Trans* 93:2147–2152. doi:[10.1039/A608564D](https://doi.org/10.1039/A608564D)
7. Schmitz G, Kolar-Anić Lj, Anić S, Grozdić T, Vukojević V (2006) Complex and chaotic oscillations in a model for the catalytic hydrogen peroxide decomposition under open reactor conditions. *J Phys Chem A* 110:10361–10368. doi:[10.1021/jp063519b](https://doi.org/10.1021/jp063519b)
8. Schmitz G, Furrow SD (2016) Bray–Liebhafsky and non-catalysed Briggs–Rauscher oscillating reactions. *Russ J Phys Chem A* 90:271–275. doi:[10.1134/S0036024415130178](https://doi.org/10.1134/S0036024415130178)
9. Vukojević V, Anić S, Kolar-Anić Lj (2000) Investigation of dynamic behavior of the Bray–Liebhafsky reaction in the CSTR. Determination of bifurcation points. *J Phys Chem A* 104:10731–10739. doi:[10.1021/jp001165x](https://doi.org/10.1021/jp001165x)

10. Pejić N, Maksimović J, Ribič D, Kolar-Anić Lj (2009) Dynamic states of the Bray–Liebhafsky reaction when sulfuric acid is the control parameter. *Russ J Phys Chem A* 83:1490–1495. doi:[10.1134/S0036024409090131](https://doi.org/10.1134/S0036024409090131)
11. Pejić N, Vujković M, Maksimović J, Ivanović A, Anić S, Čupić Ž, Kolar-Anić Lj (2011) Dynamic behavior of the Bray–Liebhafsky oscillatory reaction controlled by sulfuric acid and temperature. *Russ J Phys Chem A* 85:2310–2316. doi:[10.1134/S0036024411130231](https://doi.org/10.1134/S0036024411130231)
12. Schmitz G (1987) Cinétique de la réaction de Bray. *J Chim Phys* 84:957–965
13. Kissimonová K, Valent I, Adamčíková L, Ševčík P (2001) Numerical simulations of the oxygen production in the oscillating Bray–Liebhafsky reaction. *Chem Phys Lett* 341:345–350. doi:[10.1016/S0009-2614\(01\)00486-9](https://doi.org/10.1016/S0009-2614(01)00486-9)
14. Schmitz G, Kolar-Anić Lj, Anić SR, Čupić Ž (2008) Stoichiometric network analysis and associated dimensionless kinetic equations. Application to a model of the Bray–Liebhafsky reaction. *J Phys Chem A* 112:13452–13457. doi:[10.1021/jp8056674](https://doi.org/10.1021/jp8056674)
15. Kolar-Anić Lj, Čupić Ž, Schmitz G, Anić S (2010) Improvement of the stoichiometric network analysis for determination of instability conditions of complex nonlinear reaction systems. *Chem Eng Sci* 65:3718–3728
16. Ivanović-Šašić AZ, Marković VM, Anić SR, Kolar-Anić Lj, Čupić ŽD (2011) Structures of chaos in open reaction systems. *Phys Chem Chem Phys* 13:20162–20171. doi:[10.1039/c1cp22496d](https://doi.org/10.1039/c1cp22496d)
17. Čupić ŽD, Ivanović-Šašić A, Anić S, Stanković B, Maksimović J, Kolar-Anić LjZ, Schmitz G (2013) Tourbillon in the phase space of the Bray–Liebhafsky nonlinear oscillatory reaction and related multiple-time-scale model. *MATCH Commun Math Comput Chem* 69:805–830
18. Buchholtz FG, Broecker S (1998) Oscillations of the Bray–Liebhafsky reaction at low flow rates in a continuous flow stirred tank reactor. *J Phys Chem A* 102:1556–1559. doi:[10.1021/jp973362a](https://doi.org/10.1021/jp973362a)
19. Clarke BL (1980) Stability of Complex Reaction Networks. In: Prigogine I, Rice SA (eds) *Advances in Chemical Physics*. John Wiley & Sons Inc, New York, pp 1–215
20. Clarke BL (1988) Stoichiometric network analysis. *Cell Biophys* 12:237–253. doi:[10.1007/BF02918360](https://doi.org/10.1007/BF02918360)
21. Čupić Ž, Kolar-Anić Lj (1999) Contraction of the model for the Bray–Liebhafsky oscillatory reaction by eliminating intermediate  $I_2O$ . *J Chem Phys* 110:3951–3954. doi:[10.1063/1.478274](https://doi.org/10.1063/1.478274)
22. Čupić Ž, Kolar-Anić Lj (1999) Contraction of the complex models by the stoichiometric network analysis. In: Stojanović BD, Skorokhod VV, Nikolić MV (eds) *Advanced science and technology of sintering*. Springer, New York, pp 75–79
23. Schmitz G (1991) Etude du Braylator par la méthode de Clarke. *J Chim Phys* 88:15–25
24. Cook GB, Gray P, Knapp DG, Scott SK (1989) Bimolecular routes to cubic autocatalysis. *J Phys Chem* 93:2749–2755. doi:[10.1021/j100344a012](https://doi.org/10.1021/j100344a012)
25. Abbott JP (1977) Numerical continuation methods for nonlinear equations and bifurcation problems. *Bull Aust Math Soc* 17:307–308
26. Doedel E, Keller HB, Kernevez JP (1991) Numerical analysis and control of bifurcation problems (I): bifurcation in finite dimensions. *Int J Bifurc Chaos* 1:493–520
27. Doedel E, Keller HB, Kernevez JP (1991) Numerical analysis and control of bifurcation problems (II): bifurcation in infinite dimensions. *Int J Bifurc Chaos* 1:745–772
28. Allgower EL, Georg K (2003) *Introduction to numerical continuation methods*. SIAM
29. Kuznetsov YA (2004) *Elements of applied bifurcation theory*. Springer, New York
30. Krauskopf B, Osinga HM (2007) *Numerical continuation methods for dynamical systems—path following and boundary value problems*. Springer
31. Čupić Z, Marković VM, Ivanović A, Kolar-Anić Lj (2011) Modeling of the complex nonlinear processes: Determination of the instability region by the stoichiometric network analysis. In: Brennan CR (ed) *Mathematical modelling*. Nova Science Publishers Inc., New York, pp 111–178
32. Clarke BL, Jiang W (1993) Method for deriving Hopf and saddle-node bifurcation hypersurfaces and application to a model of the Belousov–Zhabotinskii system. *J Chem Phys* 99:4464–4478. doi:[10.1063/1.466073](https://doi.org/10.1063/1.466073)
33. Marković VM, Čupić Ž, Ivanović A, Kolar-Anić Lj (2011) The stability of the extended model of hypothalamic-pituitary-adrenal axis examined by stoichiometric network analysis. *Russ J Phys Chem A* 85:2327–2335. doi:[10.1134/S0036024411130115](https://doi.org/10.1134/S0036024411130115)
34. Čupić Ž, Marković VM, Ivanović A, Kolar-Anić Lj (2011) Modeling of the complex nonlinear processes: Determination of the instability region by the stoichiometric network analysis. In: Brennan CR (ed) *Mathematical Modeling*. Nova Science Publishers Inc., New York, pp 111–178



35. Marković VM, Čupić Ž, Vukojević V, Kolar-Anić Lj (2011) Predictive modeling of the hypothalamic-pituitary-adrenal (HPA) axis response to acute and chronic stress. *Endocr J* 58:889–904
36. Maćešić S, Čupić Ž, Kolar-Anić Lj (2012) Model of the nonlinear reaction system with autocatalysis and autoinhibition: stability of dynamic states. *Hem Ind* 66:637–646. doi:[10.2298/HEMIND120210034M](https://doi.org/10.2298/HEMIND120210034M)
37. Maćešić S, Čupić Ž, Anić S, Kolar-Anić Lj (2015) Autocatalator as the source of instability in the complex non-linear neuroendocrine model. *Int J Non-Linear Mech* 73:25–30. doi:[10.1016/j.ijnonlinmec.2014.11.008](https://doi.org/10.1016/j.ijnonlinmec.2014.11.008)
38. Maćešić SR, Čupić ŽD, Blagojević SM, Pejić ND, Anić SR, Kolar-Anić Lj (2015) Current rates and reaction rates in the stoichiometric network analysis (SNA). *Open Chem* 13:591–599. doi:[10.1515/chem-2015-0077](https://doi.org/10.1515/chem-2015-0077)